Generalized effective operator formalism for decaying systems

Marius Paraschiv, Sabine Wölk, Thomas Mannel, and Otfried Gühne

Naturwissenschaftlich-Technische Fakultät, Universität Siegen, Walter-Flex-Strasse 3, 57068 Siegen, Germany

(Received 12 July 2016; published 5 October 2016)

Systems of neutral kaons can be used to observe entanglement and the violation of Bell inequalities. The decay of these particles poses some problems, however, and recently an effective formalism for treating such systems has been derived. We generalize this formalism and make it applicable to other quantum systems that can be made to behave in a similar manner. As examples, we discuss two possible implementations of the generalized formalism using trapped ions such as ¹⁷¹Yb or ¹⁷²Yb, which may be used to simulate kaonic behavior in a quantum optical system.

DOI: 10.1103/PhysRevA.94.042103

I. INTRODUCTION

The unexpected effects of quantum correlations were initially described by Einstein, Podolsky, and Rosen (EPR) in their 1935 paper [1] as a phenomenon questioning the completeness of quantum mechanics. The natural proposal to overcome the problems raised therein was to assume the existence of hidden variables: additional parameters not present in the quantum-mechanical description, but which characterize the behavior and evolution of a quantum system.

In 1964, however, Bell [2] proposed an inequality that must be satisfied by any local hidden-variable alternative to quantum mechanics. It turns out that quantum mechanics violates this inequality, and thus no local hidden-variable theory can reproduce its full predictions. Bell's inequality was further generalized in 1969 by Clauser, Horne, Shimony, and Holt [3], and many versions of Bell-type inequalities have been proposed since then [4–6].

EPR correlations have been a research topic in the field of particle physics [7]. In particular, the system of neutral kaons exhibits interesting quantum correlations which have been studied since the discovery of kaons in the 1960s [8–10]. Due to the strangeness quantum number the neutral kaon and its antiparticle are different states, allowing for a description as a two-state system. However, due to the decay of the kaons, the time evolution of the two-state system is nonunitary. The details can be found in particle physics textbooks (see, e.g., Ref. [11]); in the context of quantum optics this has been discussed in Ref. [12].

Treating the system of neutral kaons as a two-state system allows us to draw some analogies to photons [13,14], but existing approaches suffered from a series of shortcomings [15]. The most important issues were problems with the normalization of the state of the decaying system, the difficulty of choosing an active method to measure the quasispin [16], and the difficult problem of a generalization to a higher number of particles.

In Ref. [17] the authors proposed a reformulation of the problem in terms of an effective operator formalism. Here, the time evolution of the system as well as the measurement angles can be incorporated into an effective operator that offers a series of advantages over the direct photon-analogy method: By including the nonunitary time evolution into the effective operator, one ensures that normalization is only performed with respect to the surviving particles. Another advantage is the

possibility to generalize it to an arbitrary number of particles just by the usual tensor product. Finally, an interesting property of neutral kaons, namely, the violation of *CP* symmetry, is easily included within the formalism.

In this paper, we present a generalization of this approach to general decay processes and apply it to trapped ion systems. In detail, the paper is organized as follows. In Sec. II we describe the physics of neutral kaons and the existing approaches to effective operators. In Sec. III we describe our generalized approach. Section IV presents an application to kaons and various Bell inequalities in this setting. Section V describes applications to trapped ions such as ¹⁷¹Yb or ¹⁷²Yb, which may be used to simulate kaonic behavior in quantum optics. Finally, we conclude and discuss possible further directions of research.

II. ENTANGLEMENT OF NEUTRAL KAONS

A. Neutral kaons

In this section we give a brief summary of the quantum mechanics of the neutral kaon system, which sets the stage for the further considerations. The neutral kaons are composed of a strange quark and a down antiquark, where the strange quark carries a quantum number called strangeness. Due to this quantum number we can distinguish the neutral kaon from its antiparticle:

$$|K^0\rangle = |\bar{d}s\rangle, \quad S|K^0\rangle = +|K^0\rangle, \tag{1}$$

$$|\bar{K}^0\rangle = |\bar{s}d\rangle, \quad S|\bar{K}^0\rangle = -|\bar{K}^0\rangle.$$
 (2)

The second relevant quantum number is related to the behavior of the kaons under charge conjugation C and parity P. Since the kaons are pseudoscalar particles, one obtains (making a choice for a possible arbitrary phase)

$$CP|K^0\rangle = -|\bar{K}^0\rangle,\tag{3}$$

$$CP|\bar{K}^0\rangle = -|K^0\rangle. \tag{4}$$

In particular, S and CP do not commute and hence there are no common eigenstates; in fact, we may construct the CP

eigenstates from the strangeness eigenvectors to be

$$\left|K_1^0\right\rangle = \frac{1}{\sqrt{2}}(\left|K^0\right\rangle - \left|\bar{K}^0\right\rangle),\tag{5}$$

$$\left|K_2^0\right\rangle = \frac{1}{\sqrt{2}}(\left|K^0\right\rangle + \left|\bar{K}^0\right\rangle). \tag{6}$$

Neutral kaons are produced by generating an $s\bar{s}$ pair, which hadronizes into strange particles. A particularly clean way is pursued at $DA\Phi NE$ at Frascati: The kaons are generated from the decay of a ϕ meson, which consists of two strange quarks, but is heavy enough to (exclusively) decay into a pair of neutral kaons. The ϕ meson has a definite CP quantum number and the kaon state in the moment of the decay of the ϕ (t=0) is given by

$$|\psi(t=0)\rangle = \frac{1}{\sqrt{2}}(|K^0\rangle|\bar{K}^0\rangle - |\bar{K}^0\rangle|K^0\rangle). \tag{7}$$

Kaons decay through weak interaction processes; the relevant weak transition is the decay of the strange quark into an up quark. Hence the possible final states are either two or three pions, since there is no phase space for heavier states. However, the two- and three-pion states with vanishing orbital angular momentum $\ell=0$ have different CP eigenvalues:

$$CP|\pi\pi(\ell=0)\rangle = |\pi\pi(\ell=0)\rangle,$$
 (8)

$$CP|\pi\pi\pi(\ell=0)\rangle = -|\pi\pi\pi(\ell=0)\rangle.$$
 (9)

Thus, if CP were conserved, the K_1^0 could decay exclusively to two pions, while K_2^0 could only decay into three pions. Since the phase space for the decay into three pions is much smaller than the one for the decay into two pions, the K_2^0 has a significantly longer lifetime.

Weak interactions mediate not only the decays of the kaons but also an effect called mixing. Since the K^0 and the \overline{K}^0 have common decay channels f, a K^0 state can oscillate into a \overline{K}^0 state through the process $K^0 \to f \to \overline{K}^0$. Thus the neutral kaon states undergo a mixing which in the two-dimensional space of K^0 and \overline{K}^0 is described by a Hamiltonian:

$$H = M + i\Gamma, \tag{10}$$

where M and Γ are Hermitian 2×2 matrices. Note that this Hamiltonian takes into account the decay of the kaons through the contribution of Γ , which makes the total Hamiltonian non-Hermitian

Assuming first that CP is a good quantum number, the two CP eigenstates (5) and (6) are the eigenstates of the Hamiltonian, and the eigenvalue equation reads

$$H|K_{S,L}\rangle = \lambda_{S,L}|K_{S,L}\rangle. \tag{11}$$

The eigenvalues are complex, since H is non-Hermitian. We decompose them into real and imaginary parts as

$$\lambda_{S,L} = m_{S,L} - \frac{i}{2} \Gamma_{S,L}, \tag{12}$$

where $m_{S,L}$ are the masses of the short- and long-lived states and $\Gamma_{S,L} \geqslant 0$ are the decay widths. Note that $\Gamma_S < \Gamma_L$, so Γ_S is the width of the short-lived kaon, while Γ_L is the one of the long-lived kaon. Furthermore, if CP were conserved, we would have $|K_S\rangle = |K_1^0\rangle$ and $|K_L\rangle = |K_2^0\rangle$.

The eigenvalue problem (11) is non-Hermitian, which not only leads to complex eigenvalues but also means that the eigenvectors are not orthogonal to each other. We make a choice of the relative phases of K_L and K_S as

$$\langle K_S | K_S \rangle = \langle K_L | K_L \rangle = 1, \tag{13}$$

$$\langle K_S | K_L \rangle = \langle K_S | K_L \rangle^* \geqslant 0. \tag{14}$$

Weak interactions violate the CP symmetry; in fact this was discovered in the system of neutral kaons. As a consequence, CP and H do not commute and thus the CP eigenstates (5) and (6) are not identical to the eigenstates K_L and K_S of the Hamiltonian. To this end, the eigenstates of the Hamiltonian become

$$|K_S\rangle = \frac{1}{N}(p|K^0\rangle - q|\bar{K}^0\rangle),$$

$$|K_L\rangle = \frac{1}{N}(p|K^0\rangle + q|\bar{K}^0\rangle),$$
(15)

with $N = \sqrt{|p|^2 + |q|^2}$, and only if CP is conserved we have p = q. However, CP violation is a small effect; rewriting the eigenstates of the Hamiltonian K_S and K_L in terms of the CP eigenstates K_1^0 and K_2^0 ,

$$|K_S\rangle = \frac{1}{\sqrt{1+|\epsilon|^2}} (|K_1^0\rangle + \epsilon |K_2^0\rangle),$$

$$|K_L\rangle = \frac{1}{\sqrt{1+|\epsilon|^2}} (|K_2^0\rangle + \epsilon |K_1^0\rangle),$$
(16)

we define the CP violating parameter ϵ , which has a value of approximately $\epsilon \approx 10^{-3}$. The fact that there is CP violation observed in the neutral kaon system, shown here by the nonzero ϵ parameter, leads to a slight nonorthogonality of the shortand long-lived states.

Including *CP* violation, the total time evolution of the kaon system is then given by

$$|K^{0}(t)\rangle = g_{+}(t)|K^{0}\rangle + \frac{q}{p}g_{-}(t)|\bar{K}^{0}\rangle),$$

$$|\bar{K}^{0}(t)\rangle = \frac{p}{q}g_{-}(t)|K^{0}\rangle + g_{+}(t)|\bar{K}^{0}\rangle),$$
(17)

with the time-dependent functions

$$g_{+}(t) = \frac{1}{2}(e^{-i\lambda_{S}t} + e^{-i\lambda_{L}t}),$$

$$g_{-}(t) = \frac{1}{2}(-e^{-i\lambda_{S}t} + e^{-i\lambda_{L}t}).$$
 (18)

The lifetime difference in the kaon system is substantial: The lifetimes of the two states are $\tau_S = 8.95 \times 10^{-11}$ s for the short-lived state $|K_S\rangle$ and $\tau_L = 5.11 \times 10^{-8}$ s for the long-lived state $|K_L\rangle$.

There are two physical properties of neutral kaons that make them important for our model. The first one is decay as the system is represented by the two states with different lifetimes. The second property is flavor oscillation. As the state $|\psi\rangle$ of Eq. (7) evolves in time, the particles undergo mixing, essentially an oscillation between particle and antiparticle [see Eq. (17)]. This type of behavior is known as neutral particle oscillation and will prove useful to us, as we will want to make our measurements at different times, by performing the

measurement on one particle and allowing the other to evolve for an additional time τ , before measuring. This effectively allows us to measure the spin in different directions.

B. Brief description of the effective formalism

For a system of two particles of spin 1/2, one can select four settings for the directions of the corresponding spins (two for each particle, say A_1 and A_2 for Alice's particle and B_1 and B_2 for Bob's particle). These can be used as parameters for the CHSH inequality [3]

$$\langle A_1 B_1 \rangle + \langle A_2 B_1 \rangle + \langle A_1 B_2 \rangle - \langle A_2 B_2 \rangle \leqslant 2, \tag{19}$$

where the bound is valid for local realistic theories and can be violated by quantum mechanics.

One can define a quasispin quantity, for neutral kaons, with the parametrization

$$|k_n\rangle = \cos\left(\frac{\alpha_n}{2}\right)|K_S\rangle + \sin\left(\frac{\alpha_n}{2}\right)e^{i\phi_n}|K_L\rangle,$$
 (20)

and thus give the possibility to the experimenter of choosing different quasispin directions. One must be careful though: there is no arbitrary spin direction in this case; one only has the choice of $|K_S\rangle, |K_L\rangle, |K^0\rangle, |\bar{K}^0\rangle$, due to the fact that only strangeness or lifetime measurements can be performed.

For a certain quasispin direction $|k_n\rangle$ at a certain measurement time t_n , the expectation value can be written in terms of the probability of obtaining a $|k_n\rangle$ [denoted here by Y (yes) and N (no)] as

$$E(k_n, t_n) = P(Y : k_n, t_n) - P(N : k_n, t_n)$$

= $2P(Y : k_n, t_n) - 1.$ (21)

Noteworthy is the fact that the probability $P(N:k_n,t_n)$ includes not only the case of detecting a $|k_n\rangle$ but also nondetection events.

Using our parametrization and the fact that

$$P(Y:k_n,t_n) = \text{Tr}[|k_n\rangle\langle k_n|\rho(t_n)], \qquad (22)$$

we can find an operator that satisfies the property

$$E(k_n, t_n) = \text{Tr}[O^{\text{eff}}(k_n, t_n)\rho(t=0)],$$
 (23)

where $O^{\text{eff}}(k_n, t_n)$ is called an "effective operator."

With this, the matrix form of the effective operator in the lifetime eigenbasis is

$$O^{\text{eff}} = \begin{pmatrix} \cos^2\left(\frac{\alpha_n}{2}\right)e^{-\Gamma_S t_n} - 1 & \frac{1}{2}\sin(\alpha_n)e^{i(\phi_n - \omega t_n)}e^{-\Gamma t_n} \\ \frac{1}{2}\sin(\alpha_n)e^{-i(\phi_n - \omega t_n)}e^{-\Gamma t_n} & \sin^2\left(\frac{\alpha_n}{2}\right)e^{-\Gamma_L t_n} - 1 \end{pmatrix}, \tag{24}$$

as can be constructed by following the derivations in Ref. [17], with $\omega \propto \Delta m$. Here, $\Gamma = \frac{1}{2}(\Gamma_S + \Gamma_L)$, where $\Gamma_{S,L}$ are the decay constants of the short- and long-lived states.

A few remarks are in order: First, from the matrix form of this operator, we see that for large times, when the probability that the particles have decayed is very high, the effective operator tends to minus identity. This is a reasonable expectation, since, as the particles decay, the overall amount of

detection events decreases. Second, using Eq. (23) it is easy to see that in the case of a multiparticle system the generalization is straightforward: $E = \operatorname{Tr}(O_1^{\operatorname{eff}} \otimes O_2^{\operatorname{eff}} \otimes ... \otimes O_n^{\operatorname{eff}} \rho_n)$. The experimental setup of a Bell test is rather standard:

The experimental setup of a Bell test is rather standard: a pair of particles produced at a source propagates in opposite directions. They are detected by two experimenters, by tradition named Alice and Bob. There are two possible ways to test any given Bell-type inequality in this situation: (1) fix the measurement times and measure for different quasispins and (2) fix the quasispins and measure at different times.

Because of the scarcity of directions when it comes to choosing a quasispin, the former option does not provide interesting information, other than what would be, much easier, obtained with nondecaying systems like photons. However, the decay and strangeness oscillation make the latter much more appealing. In short, both Alice and Bob agree upon a single measurement direction, say \bar{K}^0 , and each measures his or her particle at a different time.

The measurement procedure in the case of kaons also requires a certain amount of discussion: while it surely is possible to allow the particles to decay, and then identify the initial particle by its decay products (passive measurement), this does not allow the experimenter a free choice of measurement times. One possibility (active measurements) would be to insert a piece of matter in the way of the kaon beam and, thus, force the particle to decay, by interaction. The distance between the object and the kaon source would help set the measurement times. Another essential aspect is the ability of the experimenter to choose their measurement angle (in our case a choice between the particle and its antiparticle). A more detailed analysis of the various types of measurements that can be performed on kaons is given in Ref. [16].

III. GENERAL DECAYING SYSTEMS

In this section we describe our generalization of the effective operator formalism. Later, we will see how it can be applied to other systems beyond neutral kaons. This generalization is based on the Bloch equation formalism [18]. We start by treating a closed three-level system at zero temperature, with population decay from the upper two levels to a ground level (see Fig. 1). The long- and short-lived states $|K_S\rangle$ and $|K_L\rangle$ would correspond to $|2\rangle$ and $|1\rangle$, respectively. The $|0\rangle$ level plays the role of a general "decayed" level.

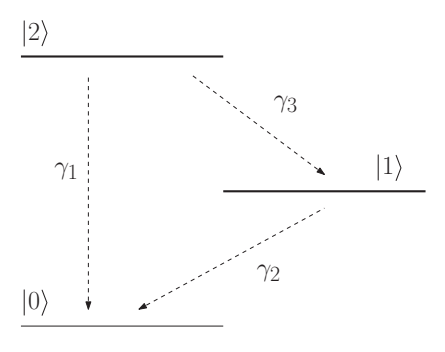


FIG. 1. A general three-level system at zero temperature with different decay processes. See the text for further details.

The time evolution of a single particle is given by the Lindblad equation

$$\dot{\rho}(t) = -i[H, \rho(t)] - \sum_{i} \gamma_{i} \left(\frac{1}{2} \{ \Lambda_{i}^{\dagger} \Lambda_{i}, \rho(t) \} - \Lambda_{i} \rho(t) \Lambda_{i}^{\dagger} \right), \tag{25}$$

with Λ_i being jump operators between different levels. Here, H is the mass term M from Eq. (10), a notation we will maintain throughout the rest of the paper. For our case, these are given by

$$\Lambda_{20} = |0\rangle\langle 2|,$$

$$\Lambda_{21} = |1\rangle\langle 2|,$$

$$\Lambda_{10} = |0\rangle\langle 1|.$$
(26)

Taking into account only the unitary part of the time evolution

$$\dot{\rho}(t) = -i[H, \rho(t)] \tag{27}$$

and denoting the density operator in column vector form as

$$\vec{\rho} = (\rho_{1,1}, \dots, \rho_{1,N}, \rho_{2,1}, \dots, \rho_{2,N}, \dots, \rho_{N,N})$$
 (28)

the unitary part becomes

$$-i[H,\rho] = -i(H \otimes \mathbb{1} - \mathbb{1} \otimes H^T)\vec{\rho}. \tag{29}$$

As for the nonunitary part of the time evolution, we simplify the notation by writing it as

$$\dot{\rho} = \frac{-\gamma}{2} (\Lambda_{+} \Lambda_{-} \rho + \rho \Lambda_{+} \Lambda_{-} - 2\Lambda_{-} \rho \Lambda_{+}), \quad (30)$$

where Λ_+ stands for Λ^{\dagger} and Λ_- stands for Λ .

Using the transformation from Eq. (29), we have

$$\begin{split} & \Lambda_{+}\Lambda_{-}\cdot\rho = (\Lambda_{+}\Lambda_{-}\otimes\mathbb{1})\vec{\rho}, \\ & \rho\cdot\Lambda_{+}\Lambda_{-} = (\mathbb{1}\otimes(\Lambda_{+}\Lambda_{-})^{T})\vec{\rho}, \\ & \Lambda_{-}\rho\Lambda_{+} = \Lambda_{-}\cdot(\rho\Lambda_{+}) = (\Lambda_{-}\otimes\mathbb{1})\cdot(\mathbb{1}\otimes\Lambda_{+}^{T})\vec{\rho}. \end{split}$$

The Lindblad equation can now be written in operator form

$$\vec{\hat{\rho}} = A\vec{\rho}.\tag{32}$$

with the time evolution operator given by the above results:

$$A = [-i(H \otimes \mathbb{1} - \mathbb{1} \otimes H^T)$$

$$-\frac{\gamma}{2}(\Lambda_+ \Lambda_- \otimes \mathbb{1} + \mathbb{1} \otimes \Lambda_+ \Lambda_- - 2\Lambda_- \otimes \Lambda_-)].$$

Note that, while for the specific way in which we have defined the Λ operator the relation $\Lambda_+^T = \Lambda_-$ holds, this is not true in general. With this, the time evolution equation of the decaying system is simply

$$\vec{\rho}(t) = e^{At} \vec{\rho}(0). \tag{33}$$

Worth mentioning is that this formulation of the time evolution also makes a numerical approach towards solving the problem possible.

The final step is to construct the general effective operator. From Eqs. (21)–(23) it follows that

$$E = \text{Tr}[2|k_n\rangle\langle k_n|\rho(t) - \rho(0)], \tag{34}$$

where we used the fact that $Tr[\rho(0)] = 1$. In order to apply the time evolution, we will write everything in vector notation

and then go back to the original matrix notation, to recover the final form of the effective operator. Denoting the matrix $|k_n\rangle\langle k_n|$ as K, we have

$$E = \text{Tr}[2(K \otimes 1)\vec{\rho}(t) - \vec{\rho}(0)]$$

= Tr[2(K \otimes 1)e^{At}\vec{\rho}(0) - \vec{\rho}(0)] (35)

[see Eq. (33)]. In vector notation, one should retain the indices from the matrix notation $(\rho_{i,j})$, in order for the trace to make sense; thus, in the above equation, the trace should be understood as

$$Tr[\vec{\rho}(t)] = \sum_{i} \vec{\rho}_{ii}(t). \tag{36}$$

Finally, we apply the exponential to \vec{K} and revert to the original matrix notation, where we replace $\vec{K}e^{At}$ with K(t):

$$E = \text{Tr}[(2K(t) - 1)\rho(0)] = \text{Tr}[O^{\text{eff}}\rho(0)], \quad (37)$$

from which one can simply identify the general effective operator as

$$O^{\text{eff}}(k_n, t_n) = 2K(k_n, t_n) - 1. \tag{38}$$

Here, the dependence of K on the time t_n and measurement direction k_n has been explicitly highlighted.

The above effective operator represents measurements performed on a single particle, and the possible settings are given by the measurement "angles" of the quasispin and the various times. Now, as previously mentioned, one can test correlations between larger numbers of particles, by taking the tensor products of the corresponding effective operators.

IV. RESULTS FOR NEUTRAL KAONS

A first test of the formalism is to apply it for the case of the CHSH inequality on two three-level quantum systems, thus also including the neutral kaon case.

Alice's settings are represented by the indices A_1 and A_2 while Bob's settings are represented by B_1 and B_2 . The witness form of the CHSH inequality is given by

$$S^{\mathrm{eff}} = O_{A_1}^{\mathrm{eff}} \otimes \left(O_{B_1}^{\mathrm{eff}} - O_{B_2}^{\mathrm{eff}}\right) + O_{A_2}^{\mathrm{eff}} \otimes \left(O_{B_1}^{\mathrm{eff}} + O_{B_2}^{\mathrm{eff}}\right),$$

and thus the test for a possible violation is simply reduced to the consideration of the maximal and minimal eigenvalues of S^{eff} , that is, the condition

$$|\operatorname{Tr}(S^{\operatorname{eff}}\rho)| \leqslant 2.$$
 (39)

In Fig. 2, we plot the relation from Eq. (39), considering the initial state of Eq. (7). While a violation is observed (compare with Ref. [13]), in order to get the optimal results, we must consider the minimal and maximal eigenvalues of the effective operator, which is the subject for the rest of this section.

Another interesting Bell-type inequality, the Sliwa-Collins-Gisin inequality, was first proposed by Sliwa [4] and shown by Collins and Gisin [5] to be nonequivalent to the original CHSH inequality. In what follows we shall denote it SCG for short.

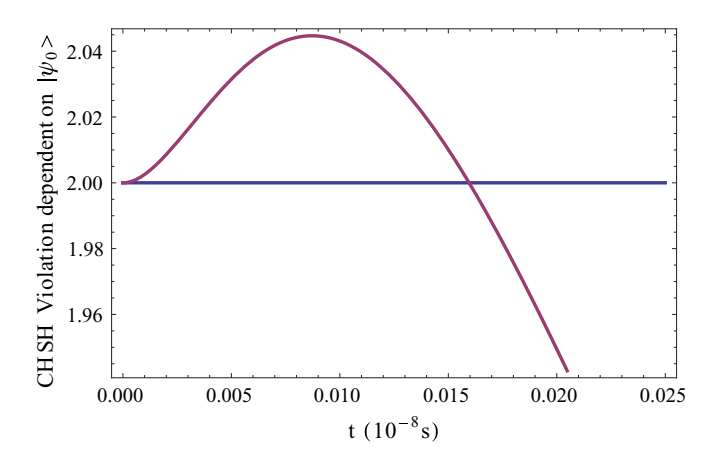


FIG. 2. Plot of Eq. (39) illustrating an obtained violation of the CHSH inequality by starting from an initial state $|\psi_0\rangle$, described in Eq. (7).

It is a three-setting inequality which is given in witness form by

$$\begin{split} \text{SCG}^{\text{eff}} &= O_{A_1}^{\text{eff}} \otimes \left(\mathbb{1} + O_{B_1}^{\text{eff}} + O_{B_2}^{\text{eff}} + O_{B_3}^{\text{eff}}\right) \\ &+ O_{A_2}^{\text{eff}} \otimes \left(\mathbb{1} + O_{B_1}^{\text{eff}} + O_{B_2}^{\text{eff}} - O_{B_3}^{\text{eff}}\right) \\ &+ O_{A_3}^{\text{eff}} \otimes \left(O_{B_1}^{\text{eff}} - O_{B_2}^{\text{eff}}\right) + \mathbb{1} \otimes \left(O_{B_1}^{\text{eff}} + O_{B_2}^{\text{eff}}\right), \end{split}$$

which must obey, for an initial two-particle state ρ ,

$$\operatorname{Tr}(\operatorname{SCG}^{\operatorname{eff}}\rho) \geqslant -4.$$
 (40)

We tested for various measurement settings, and the results can be found in Table II, in Appendix B.

It is interesting to look at the dependence of the lifetime of the violation (in units of 10 ns) in terms of ϵ (Fig. 3) and the maximal violation in terms of ϵ (Fig. 4). For the CHSH, Alice measures her fixed quasispin $|\bar{K}^0\rangle$ at time $t_{A1}=\tau,t_{A2}=0$ (in fact all measurements assume a fixed $|\bar{K}^0\rangle$ quasispin, modifying only measurement times, for both parties) and Bob measures at $t_{B1}=0,t_{B2}=\tau$. For the SCG, Alice measures at $t_{A1}=0,t_{A2}=\tau,t_{A3}=2\tau$ and Bob measures at $t_{B1}=0,t_{B2}=\tau$. Here, τ is just a plot parameter. Plots of the

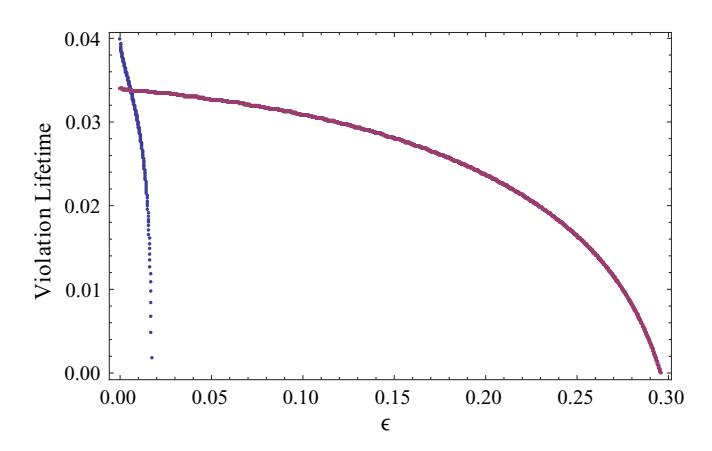


FIG. 3. Dependence of the violation lifetime, for the CHSH (fast decaying curve) and SCG (in units of 10 ns) on the *CP*-violation parameter.

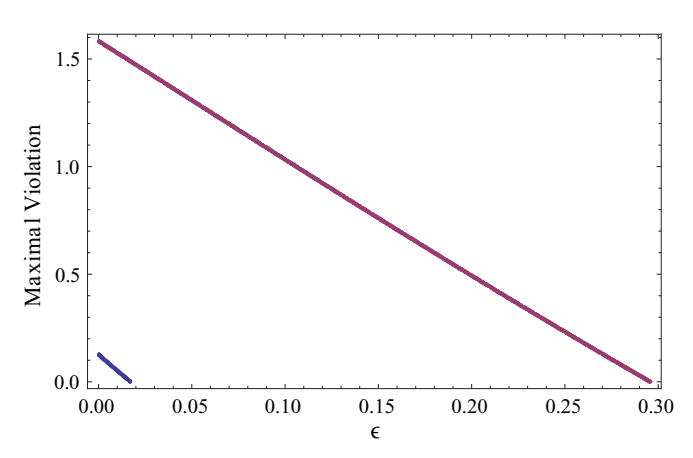


FIG. 4. Dependence of the maximal violation of the CHSH (short line) and SCG inequalities on the *CP*-violation parameter. The measurement settings are the same as for Fig. 3.

maximal and minimal eigenvalues of the effective operator, as functions of time, for different measurement settings, are shown in Table I in Appendix B.

For $\epsilon=0$ the maximal values of the effective operators were $S^{\rm eff}\approx 2.12$ and SCG^{eff} ≈ -5.58 . For $\epsilon=10^{-3}$ the value for the CHSH was $S^{\rm eff}\approx 2.11$. However, the SGC inequality showed a remarkable robustness to the variation of the *CP*-violation parameter; for values of $\epsilon=0.2$ one can still observe an effective operator eigenvalue of SCG^{eff} ≈ -4.49 (see Table II in Appendix B).

We notice that, while the presence of CP violation does reduce the amount of violation we observe, while testing Bell-type inequalities, the violation is still present for values of ϵ much larger than the one characteristic for neutral kaons.

V. SIMULATING KAONLIKE BEHAVIOR WITH TRAPPED IONS

A. General requirements

Before looking at two examples of kaonlike behavior in trapped Yb ions we summarize the general requirements for simulating kaonlike behavior with ions.

As shown in Fig. 5, there must be two levels which we identify as $|1\rangle = |K_1^0\rangle$ and $|0\rangle = |K_2^0\rangle$ and consecutively $|K_0\rangle = |+\rangle$ and $|\bar{K}_0\rangle = |-\rangle$ with $|\pm\rangle = (|0\rangle \pm |1\rangle)/\sqrt{2}$. There

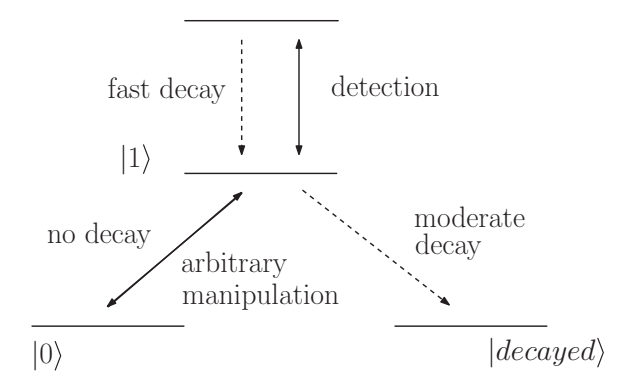


FIG. 5. Basic scheme needed to implement kaonlike behavior.

should be no decay between these two levels (as there is no decay between $|K_1^0\rangle \approx |K_S\rangle$ and $|K_2^0\rangle \approx |K_L\rangle$). Besides a two-qubit gate to create entanglement also arbitrary singe-qubit rotations (for example by using an rf field) are needed for preparation, inducing kaon oscillation and choosing arbitrary measurement directions.

Without CP violation, the oscillation between $|K^0\rangle$ and $|\bar{K}^0\rangle$ corresponds to an oscillation around the z axis given by $U(t) = \exp(-i\delta t \sigma_z)$ with the Pauli matrix σ_z . The rotation frequency δ is given by the detuning $\delta = \omega_K - \omega_L$ between the level splitting ω_K and the reference laser ω_L determining the rotating reference frame.

The CP violation ε leads to several effects. For example $|K^0(t)\rangle$ is decaying faster than $|\bar{K}^0(t)\rangle$ and the decay rates for both states start to oscillate. Furthermore their expectation values $\langle \sigma_z(t) \rangle$ undergo small oscillations and we find $\langle \sigma_z(t) \rangle_{\bar{K}^0} \geqslant \langle \sigma_z(t) \rangle_{\bar{K}^0}$ for all times. This behavior can be simulated by slightly tilting the rotation axis. The connection between the CP violation and the tilting is given by

$$\frac{\delta}{\sqrt{\delta^2 + \Omega^2}} = \frac{1 - \varepsilon}{1 + \varepsilon} \tag{41}$$

with the Rabi frequency Ω determining the strength of the laser or microwave.

Two additional levels are needed, one for fluorescence detection (from which a fast decay must exist to one of the qubit states) and another, representing the state of decay products, with a moderate decay rate Γ_S from one of the two qubit states.

In general, arbitrary values for the oscillation frequency ω , the decay rate Γ_S , and the CP violation ε can be chosen for our ion system. However, the behavior of the here-described ion system mimics kaonlike behavior only for small values of the CP violation, that is, $\varepsilon \ll \omega/\Gamma_S$. This becomes apparent if we look at Eqs. (17) and (18), which lead to unphysical behavior for large ε .

B. Examples

In this final section we present two possible ways to simulate decaying systems with quasikaon behavior using trapped Yb ions. We will only briefly go over the examples here. For a more detailed description see the Appendix.

Example 1. The first proposal is based on the level structure of $^{171^+}$ Yb sketched in Fig. 6. The qubit is defined as $|0\rangle = |S,F=0\rangle$ and $|1\rangle = |S,F=1,m_F=1\rangle$ and the decayed state is represented by $|S,F=1,m_F=0\rangle$ and $|S,F=1,m_F=-1\rangle$. $|0\rangle$ and $|1\rangle$ are both long-lived states. However, decay can be generated by weak driving of the $|S,F=1,m_F=1\rangle \leftrightarrow |P,F=0\rangle$ transition with σ^- polarized light. From $|P,F=0\rangle$ the state decays fast to all $|S,F=1,m_F\rangle$ states. It is important to note here that the strength of the decay is thus tunable, by tuning the strength or duration of the transitions.

This decay behavior is slightly different from kaons, because $|0\rangle$ does not decay and there is a nonzero probability of $|1\rangle$ "decaying" to itself, which leads to dephasing. More clearly, while for neutral kaons one could express the decay process as

$$\Gamma = \gamma_S |\text{decayed}\rangle\langle 1| + \gamma_L |\text{decayed}\rangle\langle 0|, \tag{42}$$

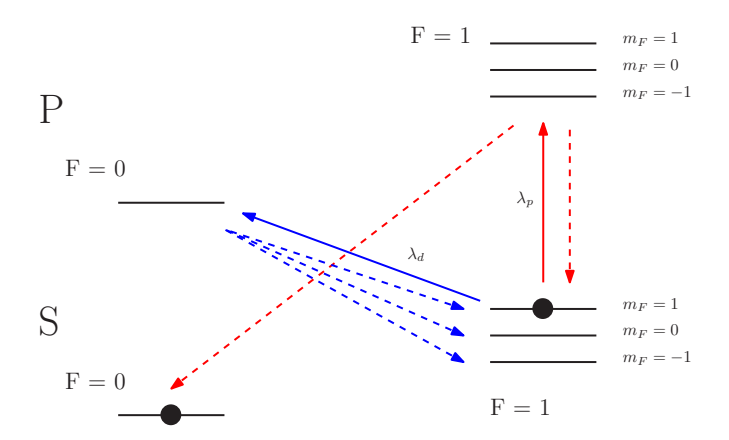


FIG. 6. An implementation of the effective formalism using ¹⁷¹⁺Yb. The qubit is defined between the two levels marked with thick dots.

where, for clarity of notation, the short-lived kaon state has been identified with $|1\rangle$ and the long-lived kaon state has been identified with $|0\rangle$, the case for example 1 is described by

$$\Gamma' = \gamma_S(\frac{2}{3}|\text{decayed}\rangle\langle 1| + \frac{1}{3}|1\rangle\langle 1|), \tag{43}$$

where there is always a chance of decay to the initial level (dephasing). In Fig. 7 we plot the violation lifetimes in terms of the CP-violation parameter with and without splitting γ_S into 2/3 decay and 1/3 dephasing.

Another necessary step to simulate the kaon is to generate entanglement between two ions. This is achieved in our example by using magnetic gradient-induced coupling (MAGIC) [19,20].

State detection of the ion is achieved by a single-qubit rotation to choose the measurement direction and consecutively driving the $|S,F=1\rangle \leftrightarrow |P,F=0\rangle$ transition with unpolarized light and detecting the scattered photons. Unfortunately, this state-dependent fluorescence measurement is only able to distinguish between the states $|S,F=0\rangle$ and $|S,F=1\rangle$, but cannot resolve the sublevels $|m_F=0/\pm 1\rangle$.

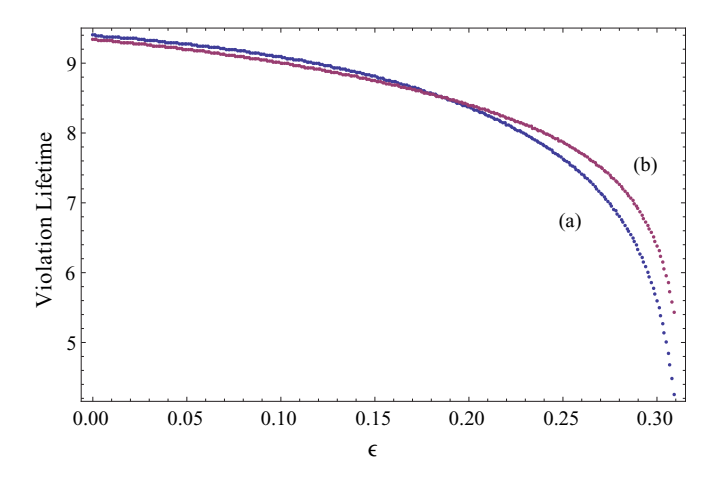


FIG. 7. The effect of dephasing on the violation lifetimes (units of 10 ns) for the SCG inequality, in terms of ϵ . Here we plot both the case of (a) only decay with strength γ_S and (b) splitting γ_S into 2/3 decay and 1/3 dephasing.

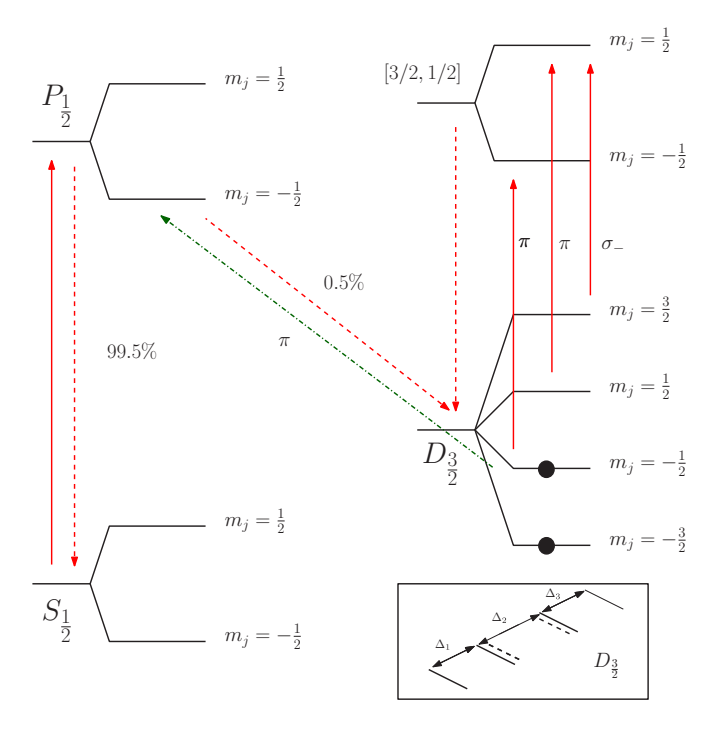


FIG. 8. An implementation of the effective formalism using ¹⁷²Yb⁺. The qubit is defined between the two levels marked with thick dots. The effect of the ac Stark shift is also shown in the lower box.

Therefore, each probability measured in such a way will correspond to the sum of the probability $P(|k_n\rangle)$ to be in the state $|k_n\rangle$ plus the probability that the ion or kaon has already decayed. Therefore, instead of measuring $P(|\bar{K}_0\rangle)$ we rotate $|K_0\rangle = |+\rangle$ onto the state $|1\rangle$ and perform in this way an inverse measurement and determine the probability $P = 1 - P(|\bar{K}_0\rangle)$. That is, instead of asking "What is the probability corresponding to the state $|\bar{K}^0\rangle$?", we may equivalently ask "What is the probability for not obtaining $|\bar{K}_0\rangle$?".

Example 2. The second example comes to eliminate the dephasing problems one finds with the first. This time, we use $^{172^+}$ Yb ions (see Fig. 8). The qubit is defined as $|0\rangle = |D_{3/2}, m_i = -3/2\rangle$ and $|1\rangle = |D_{3/2}, m_i = -1/2\rangle$.

To simulate decay, we drive the $|D_{3/2},m_j=-1/2\rangle \leftrightarrow |P,m_j=-1/2\rangle$ transition with π -polarized light. From $|P,m_j=-1/2\rangle$ the ion decays with over 99% probability into the $|S,m_j=\pm 1/2\rangle$ state and not back into the $|D_{3/2},m_j=-1/2\rangle$. Similar to the first example, we perform again an inverse measurement by transferring $|K^0\rangle$ onto $|P,m_j=-1/2\rangle$.

Two remarks need to be made here. First, the time evolution of "decay" and "oscillation" commutes only for $\varepsilon=0$. In this case, we are able to switch on the lasers or microwaves causing the decay and the oscillation one after the other. However, for $\varepsilon\neq0$ our way to model interferes with the oscillation. Therefore, we have to use the Trotter theorem and we approximated the time evolution by switching between oscillation and decay in short time intervals. This is a standard method in digital quantum simulations and the approximation can be made arbitrarily good by shortening, e.g., the time intervals (see, e.g., [21]).

Second, as explained above, there are different decay channels between kaons and the chosen ion examples [compare Eqs. (42) and (43)]. This does not significantly modify the nature results for small CP violations ϵ as depicted in Fig. 7.

VI. CONCLUSION

We have described an easy-to-use formalism that facilitates the study of entanglement for systems under nonunitary time evolution. Besides decay, the systems chosen also display an oscillation between two orthogonal states, raising the interesting possibility of performing the bipartite measurements at different times. The generalized formalism was applied to neutral kaons, in order to show that it does indeed reproduce previous results, and then applied to the case of two ytterbium isotopes, ¹⁷¹Yb and ¹⁷²Yb. The purpose of the latter is to exemplify a similar type of behavior, which comes naturally for kaons, on a different but practically relevant system, the motivation given by the fact that trapped ions are an important implementation for quantum computation in particular and quantum information processing in general.

The treatment of entanglement in unstable systems can provide a new way of studying the predictions of quantum mechanics in systems other than kaons and ions. The behavior treated above can be reproduced with other systems, for example photons traveling through optical fibers. In this case birefringence determines fast and slow polarization modes, an analog of the long- and short-lived states of neutral kaons, and polarization dependent loss is an analog to the decay property [14].

Meson-antimeson systems exhibit one interesting feature that does affect the amount of violation one observes in Bell-type inequalities, the phenomenon of *CP* violation. Because *CP* violation translates into an asymmetry between matter and antimatter the eigenstates of the system's Hamiltonian become slightly nonorthogonal (due to the different probabilities corresponding to the states representing the particle and its antiparticle). Such behavior can also be simulated in the case of trapped ions by a detuned laser/rf-pulse driving the kaon-antikaon oscillation. Another essential feature of the formalism is that it allows for an analytical method to be applied [see Eq. (33)], because it reduces the entire time evolution of the system to exponentiating one single operator that encompasses both unitary and nonunitary time evolution.

For future research, it would be desirable to use the formalism for other systems where decay or no-detection events play a role, such as polarized photons. Then, the formalism can be combined with other tools in entanglement theory, such as entanglement witnesses. This may open a way for entanglement characterization and quantification in the presence of noise and imperfect detectors.

ACKNOWLEDGMENTS

We thank Ali Asadian and Michael Johanning for the useful discussions and suggestions. This work has been supported by the FQXi Fund (Silicon Valley Community Foundation), the Deutsche Forschungsgemeinschaft Research Unit FOR 1873, and the European Research Council (Consolidator Grant No. 683107/TempoQ).

APPENDIX A

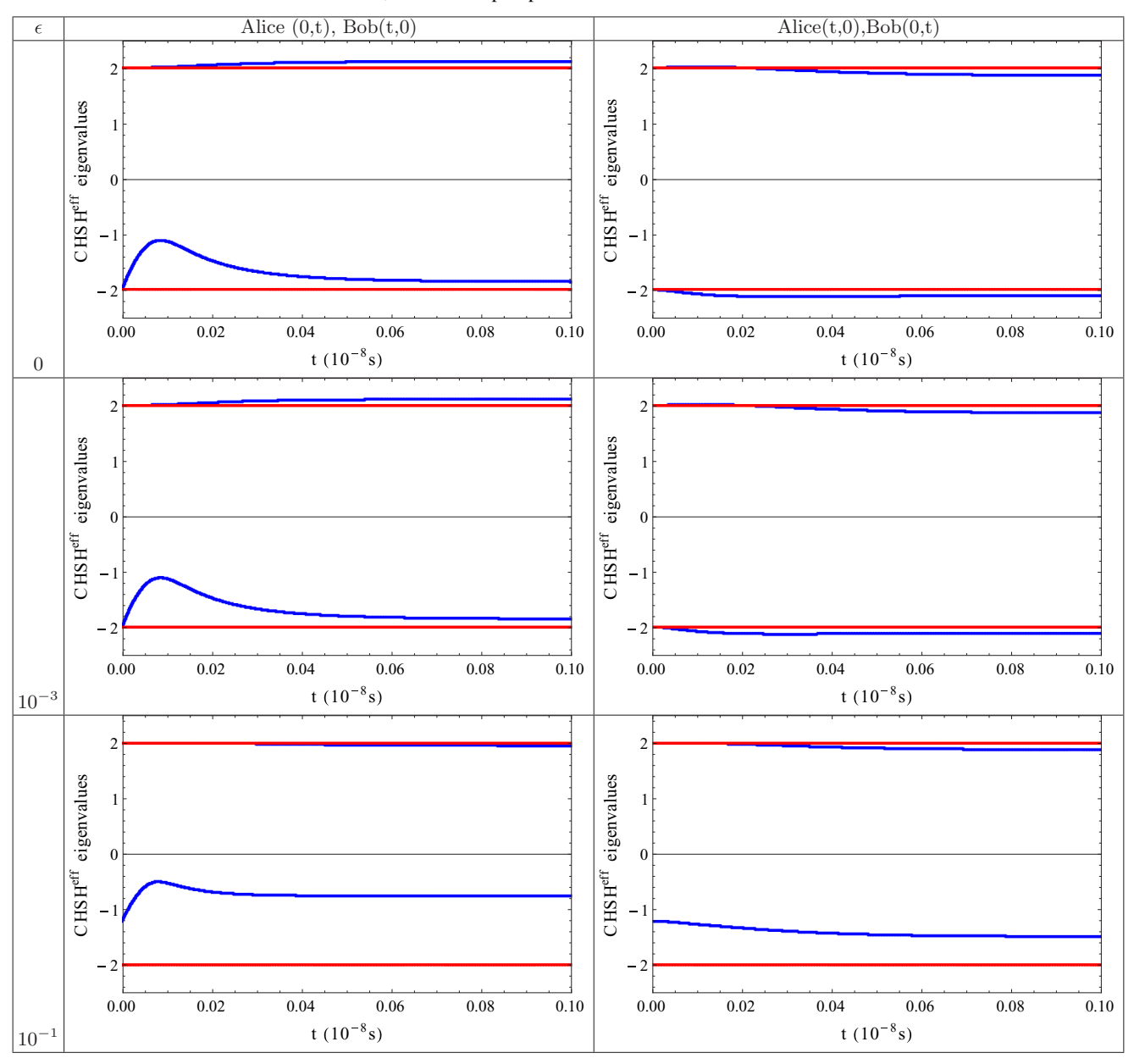
Example 1. The first example (Fig. 6) uses $^{171^+}$ Yb ions. The qubit is defined here between $|S, F = 0\rangle = |0\rangle$ and $|S, F = 1, m_F = 1\rangle = |1\rangle$ (highlighted in the figure by thick dots).

The initialization is done by driving an unpolarized pumping laser, λ_P between the F=1 levels, of S and P, and a consecutive decay to the $|S,F=0\rangle$ state. The arbitrary rotation in the qubit basis $\{|0\rangle,|1\rangle\}$ is performed via a polarized rf field. In this way, any superposition of $|0\rangle$ and $|1\rangle$ can be prepared. This also assures that a readout is possible in any basis (corresponding to a rotation from the $\{K_S,K_L\}$ to the $\{K^0,\bar{K}^0\}$, in the kaon case).

The decay is simulated by a second polarized laser λ_d driving the transition $|S,F=1,m_F=1\rangle \leftrightarrow |P,F=0\rangle$. From $|P,F=0\rangle$, the ion decays very fast into the $|S,F=1\rangle$ levels, the probabilities for each of the $m_F=0,\pm 1$ are equal. This essentially turns the $|F=1,m_F=0\rangle$ and $|F=1,m_F=-1\rangle$ sublevels into a generalized decayed state (the third state in our kaon formalism). There is an inconvenience here, however. Due to the equal probability of a decay from the P level back to any of the three $|S,F=1\rangle$ sublevels, one also gets dephasing. We will see in the second example how this problem can be overcome.

The essence of the effective formalism is that it does not distinguish between a nondetection event and one of the two

TABLE I. Plots (for neutral kaons) for the minimal and maximal eigenvalues of the CHSH effective operator, represented here in blue (dark gray), for certain values of the *CP*-violation parameter. The red (light gray) lines represent the classical limits of the CHSH inequality. The settings are for both Alice and Bob measuring at different times; for example, A(0,t) means Alice's first measurement is made at $\tau = 0$ and the second measurement is made at $\tau = t$, where t is a plot parameter.



possible states (decayed or $|K^0\rangle$, when measuring $|\bar{K}^0\rangle$, in the kaon case). This could be translated into

$$\underbrace{P_{|\bar{K^0}\rangle}}_{P(Y)} + \underbrace{P_{|K^0\rangle} + P_{\text{decayed}}}_{P(N)} = 1. \tag{A1}$$

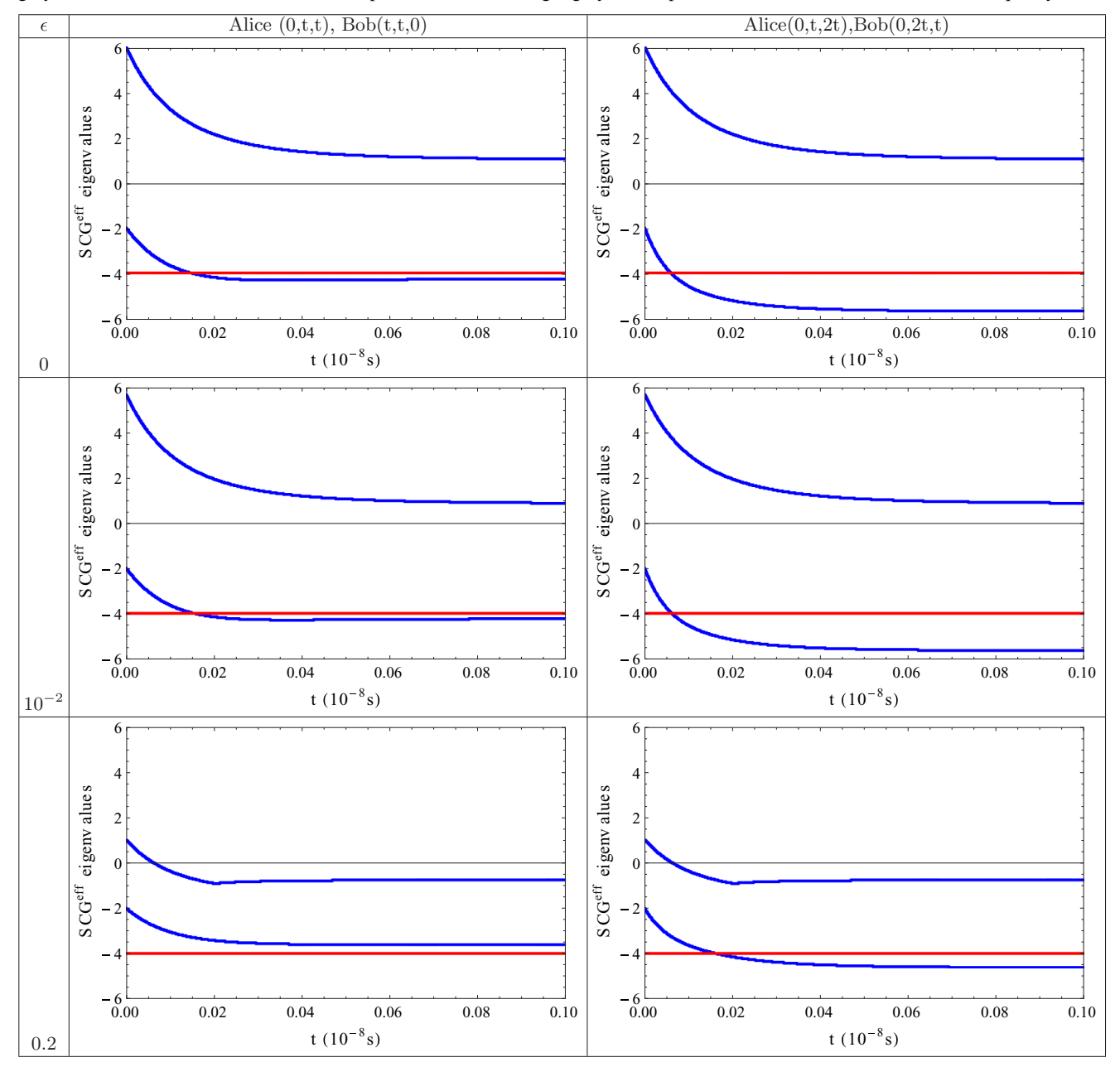
This provides the option of performing the opposite measurement (corresponding to P(N) above). For this, we perform a population inversion between the $|S,F=1\rangle$ sublevels and the $|S,F=0\rangle$ level. Then, a typical fluorescence measurement can be performed on the S level. There is also a second option to perform the population inversion and that is a population shelving from the two sublevels, representing the decayed state, to some other atomic level.

Example 2. A second way to implement the formalism is to use 172 Yb⁺ ions. In this case, the qubit is defined between the $|D_{3/2},m_j=-3/2\rangle$ and $|D_{3/2},m_j=-1/2\rangle$ levels (Fig. 8).

The implementation is done by running a pump laser between the S and P states; this leads to a population transfer to all four $D_{3/2}$ sublevels, due to decay. Then a combination of π and σ_- polarized lasers moves the populations of the upper three D sublevels to the $|[3/2,1/2]\rangle$ states, and ultimately to the $|D_{3/2},m_i|=-3/2\rangle$ sublevel.

Coherent driving of the $|D_{3/2},m_j=-3/2\rangle \leftrightarrow |D_{3/2},m_j=-1/2\rangle$ transition causes a problem, because the level splittings of all $|D_{3/2}\rangle$ states are equal. To isolate this transition, an ac Stark shift is induced, to increase the distance between the qubit levels and the sublevels $m_j=1/2$ and 3/2.

TABLE II. Plots (for neutral kaons) for the minimal and maximal eigenvalues of the SCG effective operator, represented here in blue (dark gray), for certain values of the *CP*-violation parameter. The red (light gray) line represents the classical limit of the SCG inequality.



The decay is modeled by a weak pulse driving the transitions $|D_{3/2}, m_i = -1/2\rangle \leftrightarrow |P_{1/2}\rangle$.

Finally, we transfer again the state $|K^0\rangle$ onto $|P\rangle$ before performing a state-dependent fluorescence measurement by driving the $|S\rangle \leftrightarrow |P\rangle$ transition. This measurement is again an inverse measurement similar to the first example, essentially measuring the probability $1 - P(\bar{K}^0)$ (using kaon notation).

In both examples, two ions can be entangled with the help of MAGIC [19,20] to generate a bipartite system with similar properties as pairs of neutral kaons.

APPENDIX B

The suggested implementations of the effective formalism allow for one to tune the value of the quasi-CP-violation parameter ϵ . This value has a direct impact on the observed violation of a Bell inequality. We reproduce here the minimal and maximal eigenvalues of the effective operators, corresponding to the CHSH and SCG inequalities, for various values of ϵ , as functions of time. Two different measurement settings have been chosen for Alice and Bob, in both cases. The results are shown in Table I and II.

- [1] A. Einstein, B. Podolsky, and N. Rosen, Phys. Rev. 47, 777 (1935).
- [2] J. S. Bell, Physics 1, 195 (1964).
- [3] J. F. Clauser, M. A. Horne, A. Shimony, and R. A. Holt, Phys. Rev. Lett. 23, 880 (1969); 24, 549 (1970).
- [4] C. Sliwa, Phys. Lett. A 317, 165 (2003).
- [5] D. Collins and N. Gisin, J. Phys. A 37, 1775 (2004).
- [6] N. Brunner, D. Cavalcanti, S. Pironio, V. Scarani, and S. Wehner, Rev. Mod. Phys. 86, 419 (2014).
- [7] S. Banerjee, A. K. Alok, and R. MacKenzie, Eur. Phys. J. Plus 131, 129 (2016).
- [8] D. R. Inglis, Rev. Mod. Phys. 33, 1 (1961).
- [9] T. B. Day, Phys. Rev. 121, 1204 (1961).
- [10] H. J. Lipkin, Phys. Rev. 176, 1715 (1968).
- [11] O. Nachtmann, *Elementary Particle Physics: Concepts and Phenomena* (Springer, New York, 1990).
- [12] R. A. Bertlmann and B. C. Hiesmayr, Phys. Rev. A 63, 062112 (2001).

- [13] N. Gisin and A. Go, Am. J. Phys. **69**, 264 (2001).
- [14] A. Go, J. Mod. Opt. 51, 991 (2004).
- [15] R. A. Bertlmann, A. Bramon, G. Garbarino, and B. C. Hiesmayr, Phys. Lett. A 332, 355 (2004).
- [16] A. Bramon, G. Garbarino, and B. C. Hiesmayr, Phys. Rev. A 69, 062111 (2004).
- [17] A. Di Domenico, A. Gabriel, B. C. Hiesmayr, F. Hipp, M. Huber, G. Krizek, K. Mühlbacher, S. Radic, Ch. Spengler, and L. Theussl, Found. Phys. 42, 778 (2012).
- [18] F. Bloch, Phys. Rev. 70, 460 (1946).
- [19] F. Mintert and Ch. Wunderlich, Phys. Rev. Lett. **87**, 257904 (2001); **91**, 029902(E) (2003).
- [20] M. Johanning, A. Braun, N. Timoney, V. Elman, W. Neuhauser, and C. Wunderlich, Phys. Rev. Lett. 102, 073004 (2009).
- [21] B. P. Lanyon, C. Hempel, D. Nigg, M. Müller, R. Gerritsma, F. Zähringer, P. Schindler, J. T. Barreiro, M. Rambach, G. Kirchmair, M. Hennrich, P. Zoller, R. Blatt, and C. F. Roos, Science 334, 57 (2011).